International Journal of Technology

http://ijtech.eng.ui.ac.id

Research Article

Design Concept of Fiber Optic Bending Sensor using Incohrent Optical Frequency Domain Reflectometry and Two Photon Absorption Process in Avalanche Photodiode

Yuta Kurihara[1], Shinta Tsuzuki[1], Takuma Serizawa[2], Yosuke Tanaka[1*]

[1]Graduate School of Engineering, Department of Biomedical Engineering, Tokyo University of Agriculture and Technology, 2-24-16 Nakacho Koganei-shi Tokyo-to, 184-0012, Japan

[2]Graduate School of Engineering, Tokyo University of Agriculture and Technology, 2-24-16 Nakacho Koganei-shi Tokyo-to, 184-0012, Japan

*Corresponding author: tyosuke@cc.tuat.ac.jp; Tel.: +81-42-388-7405

Abstract: In various fields, bending sensors based on optical fibers have gained significant attention. These include structural health monitoring and shape measurement of medical devices such as catheters. The characteristics of fibers, such as thinness, flexibility, light weight, and immunity to electromagnetic interference, make them suitable for various applications. Among various techniques, fiber Bragg grating (FBG) sensors are widely employed to measure strain through shifts in their reflection spectra, which are proportional to the applied strain. A single FBG can only measure the strain along one direction. In contrast, multicore fibers with Bragg gratings inscribed in multiple cores enable directional bending sensing by comparing the spectral shifts of peripheral cores against the central core. However, it is challenging to simultaneously measure overlapping reflection spectra from multiple cores using a single photodetector. Conventional approaches employ broadband light sources or wavelength-tunable lasers with multiple photodetection units, resulting in complex systems. In this study, we propose a novel method for spectral separation and identification that utilizes incoherent optical frequency domain reflectometry (I-OFDR) and the two-photon absorption (TPA) process of a silicon avalanche photodiode (Si-APD). I-OFDR uses laser light whose intensity is modulated by a chirped signal. The TPA photocurrent enables I-OFDR signal detection without the need for complex electrical circuitry. A key advantage of the proposed system is its fast measurement capability: in our proof-of-concept experiment, the measurement was completed in 25 s, which is significantly shorter than the several minutes typically required by our conventional methods. The system design and preliminary experimental results validate the feasibility and efficiency of the proposed approach.

Keywords: Bending sensor; Fiber sensor; Incoherent optical frequency domain reflectometry; Two-photon absorption

1. Introduction

Optical fiber-based sensing technologies have attracted considerable attention across various fields due to their inherent advantages such as thinness, light weight, and immunity to electromagnetic interference of an optical fiber (Lyu et al., 2025; Madani et al., 2023; Nor et al., 2023; Zhu et al., 2022 ; He and Liu, 2021; Pevec and Donlagić, 2019; H. Li et al., 2004; Hochberg, 1986). These features make them particularly suitable for applications in structural health monitoring of civil infrastructure (Riza et al., 2020) and shape sensing in medical devices (Ben Hassen et al., 2023; Issatayeva et al., 2021; Wei and Jiang, 2021; Henken et al., 2014; Roesthuis et al., 2014) such as catheters (Ben Hassen et al., 2023) and endoscopes (Vilches et al., 2023). Among these technologies, fiber Bragg grating (FBG) sensors (You et al., 2025;

https://doi.org/10.14716/ijtech.v17i1.8194
Received July 2025; Revised November 2025; Accepted November 2025

Roesthuis et al., 2014; Kersey et al., 1997; Hill and Meltz, 1997) are widely used for multipoint sensing, including strain and temperature.

In recent years, bending sensing using FBGs (Yue et al., 2023; L. Li et al., 2021; Fujiwara et al., 2019; Liu et al., 2019; James et al., 2016) and other grating structures (Allsop et al., 2006; Liu et al., 2000) has emerged as a promising technique for detecting curvature, particularly in applications requiring flexible and electromagnetic noise-resistant sensing, such as robotic motion tracking (Wang et al., 2016) and biomedical shape reconstruction. While a single FBG can only measure strain along one axis, multicore fibers with Bragg gratings inscribed in multiple cores enable directional bending detection by comparing the Bragg wavelength shifts with each other cores (Yang et al., 2022; Budnicki et al., 2020; Khan et al., 2019; Barrera et al., 2015; Moore and Rogge, 2012). However, the simultaneous measurement of overlapping reflection spectra from multiple Bragg gratings typically requires specially designed gratings, multiple detection units, or an optical switching system (Donko et al., 2018; Lindley et al., 2014; Flockhart et al., 2003). Achieving this with a single photodetector would greatly simplify the overall system architecture.

To address this issue, our research group has been investigating a novel approach that utilizes intensity correlation measurements based on the two-photon absorption (TPA) process in a silicon avalanche photodiode (Si-APD) (Tsuzuki et al., 2024; Sato et al., 2022; Sonoda et al., 2021;Tanaka et al., 2019; Tanaka and Miyazawa, 2017; Tanaka et al., 2017). This method enables the spatial separation and identification of multiple FBG spectra based on their relative positions. The positions of the FBGs are identified by sweeping the modulation frequencies of the intensity-modulated probe and reference beams. Additionally, the probe laser wavelength is swept to measure the reflection spectra of the FBGs.

In our previous method, step-by-step modulation frequency scanning was performed, allowing precise and long-distance measurement, but at the cost of increased measurement time. Recently, we demonstrated a faster technique using incoherent optical frequency domain reflectometry (I-OFDR) combined with the TPA process in a Si-APD (Sato et al., 2022). Although the measurable distance range in I-OFDR is limited, it significantly reduces the measurement time. In this study, we propose a system that applies this technique to a fiber-optic bending sensing system. In this system, the measurement can be completed within a few tens of seconds, which is significantly faster than the several minutes required in the previous methods. We demonstrate its feasibility through system design and preliminary experiments. Our approach offers a simplified and scalable solution for high-resolution, direction-sensitive bending sensing.

2. Methods

2.1 Two-photon absorption process in silicon avalanche photodiode

In silicon photodiodes and avalanche photodiodes (Si-APDs), the photocurrent is proportional to the optical power of visible light, where the silicon bandgap is overcome by one photon energy. The Si-APD used in our experiment has a sensitivity to the light with a wavelength in the range of 400–1000 nm. On the other hand, the Si-APD is generally insensitive to the light with a wavelength of 1.55 μm. However, high-intensity 1.55 μm light can induce the TPA process and generate a photocurrent (Figure 1). In the TPA process, the silicon bandgap is overcome by the two-photon energy. Suppose that the probability of excitation to the virtual state in the middle of the bandgap by a single photon is P, the probability of excitation to the excited state is proportional to P^2. Consequently, the photocurrent generated by TPA is proportional to the square of the incident light intensity, allowing for optical signal intensity correlation measurements.

2.2 Incoherent optical frequency domain reflectometry (I-OFDR)

I-OFDR is a technique that uses intensity modulation with a repetitive chirped signal, as illustrated in Figure 2(a). Unlike our previous methods, which employed step-by-step frequency

scanning, I-OFDR enables faster measurements by sweeping modulation frequencies over tens of MHz. The performance depends on the function generator used in the system, but MHz-order modulation is achievable. The chirped signal frequency F(t) is characterized by its center frequency F_c, frequency deviation F_d, and modulation frequency F_m.

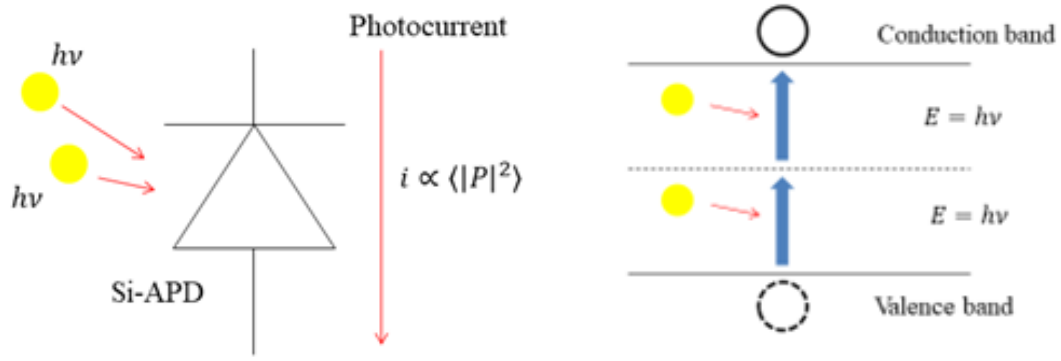

(a) (b)

Figure 1 (a) Illustration of the two-photon absorption (TPA) process in Si-APD; and (b) conceptual figure of the carrier excitation

When the intensity-modulated probe light propagates through an optical fiber of length ΔL, it experiences a time delay τ given by the following:

$$\tau = n\ c\ \Delta L \tag{1}$$

where ^{n} is the effective refractive index of the optical fiber, and c is the speed of light in vacuum. In I-OFDR, the intensity of the reference light is modulated with the same chirped signal applied to the probe light. Since the propagation time difference between the probe and the reference is τ at the signal detection unit, the modulation frequency difference F_{beat} in Figure 2(b) is given as follows:

$$F_{beat} = 2\ F_d\ F_m\ \tau = \frac{2\ n\ F_d\ F_m\ \Delta L}{c} \tag{2}$$

In the conventional I-OFDR system, the beat frequency is obtained by detecting the probe and reference signals separately using different photodetectors and multiplying the O/E converted signals. However, as explained in the next section, the use of the TPA process in a Si-APD enables direct optical correlation detection, significantly simplifying the system architecture.

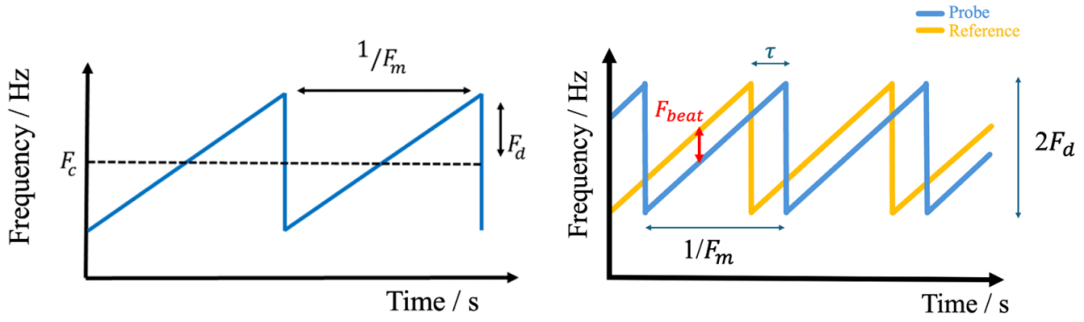

(a) (b)

Figure 2 (a) Chirped signal frequency for the intensity modulation of the optical probe and reference signals; and (b) modulation frequency of the probe and reference light in the I-OFDR system

2.3 I-OFDR with TPA in Si-APD

The optical intensities of the probe and reference beams at the Si-APD surface can be described as follows:

$$I_p(t) = I_p\,[1 + \phi_I cos\ \{2\pi\ f_I(t-\tau)\}]\,[1 + \phi_p cos\{2\pi f(t-\tau)\cdot(t-\tau)\}] \tag{3}$$

$$I_r(t) = I_r\,[1 + \phi_r cos\{2\pi f(t)t\}] \tag{4}$$

where I is the optical intensity, ν is the optical frequency, f is the chirped signal frequency, f_I is the modulation frequency for lock-in detection, ϕ is the modulation index, n is the refractive index, and c is the speed of light. Subscripts p, r, and I are associated with the probe, reference, and lock-in detection, respectively.

For simplicity, we assume the chirped signal frequency to be

$$f(t) = 2F_d\ F_m\ t\ +\ F_0 \tag{5}$$

The chirped signal in the actual system is periodic, resulting in two types of beat frequencies F_{beat} □. However, the higher beat frequency signal is not required and is removed during signal processing. Therefore, this simplified assumption does not affect the validity of the analysis.

When the probe and reference lights are incident on the Si-APD and the TPA process is induced, a photocurrent proportional to the mean square of the incident optical intensity is generated. By using an appropriate load for the Si-APD to make the time constant much longer than $1/F_m$ but shorter than $1/\tau$, the TPA photocurrent is given by

$$i_{TPA}\ \alpha\ \left\langle |I_p(t-\tau) + I_r(t)|^2 \right\rangle = \left\langle |I_p(t-\tau)|^2 + |I_p(t)|^2 + 2I_p(t-\tau)I_r(t) \right\rangle \tag{6}$$

where the square bracket $\langle\rangle$ denotes the time average. The TPA signal detected by the lock-in amplifier is

$$i_{TPA}\ \alpha\ (DC\ term) + cos2\pi\ f_{beat}\ t \tag{7}$$

The reflection points are measured from the beat signal frequency.

2.4 Bending measurement using multicore FBG (MCFBG)

Figure 3(a) shows a cross-sectional view of the MCFBG used in this study. The central core is evenly surrounded by six peripheral cores. To define the reference plane for the bending direction, we consider a plane passing through the midpoint between cores 1 and 6 and the midpoint between cores 3 and 4, as shown by the dashed line. The solid line indicates the actual bending plane, which is rotated from the reference plane by θ_B. The angle between the reference plane and the plane containing the central and individual cores is denoted as θ_j (j = 1, 2, ..., 6). The perpendicular distance from each core to the bending plane is denoted as r_j (j = 1, 2, ..., 6). As the strain applied to each core increases, r_j also increases. This distance r_j can be expressed in terms of the distance r between the peripheral and central cores and the angular difference between the bending and reference planes. Therefore, the strain ε_j applied to each core is given by the following equation:

$$\varepsilon_j = \frac{r_j}{R}\ +\ \varepsilon_{j0} = Kr\ sin\ (\theta_j - \theta_B)\ +\ \varepsilon_{j0} \tag{8}$$

where ε_{j0} is the initial strain, R is the bending radius, and $K = 1/R$ is the curvature.

When the optical fiber is bent, the outer region undergoes tensile strain, whereas the inner region experiences compression. The central core remains unaffected by the strain due to its

position at the neutral axis. Therefore, the Bragg wavelengths shift differently, depending on whether the core is located in the center, outer, or inner region.

Figure 3(b) plots the Bragg wavelength shifts against the angular positions of each core, using polar coordinates with the central core as the origin. These data points can be fitted with a sinusoidal curve. In this model, the sinusoidal function amplitude corresponds to the curvature, and the initial phase represents the bending direction.

Let S be the strain sensitivity coefficient, $\Delta\varepsilon$ the applied strain on the FBG, K the temperature sensitivity coefficient, and ΔT the temperature change. Then, the Bragg wavelength shift of the FBG can be expressed as:

$$\Delta\lambda_B = S\Delta\varepsilon + K\Delta T \tag{9}$$

When strain is applied to a multicore FBG with no temperature change, the Bragg wavelength shift for core j is derived from Equation (9) as:

$$\Delta\lambda_{Bj} = S(\varepsilon_j - \varepsilon_{j0}) \tag{10}$$

Using Equations (8) and (10), the curvature R and bending direction θ_B can be obtained by measuring the difference in the Bragg wavelengths before and after bending.

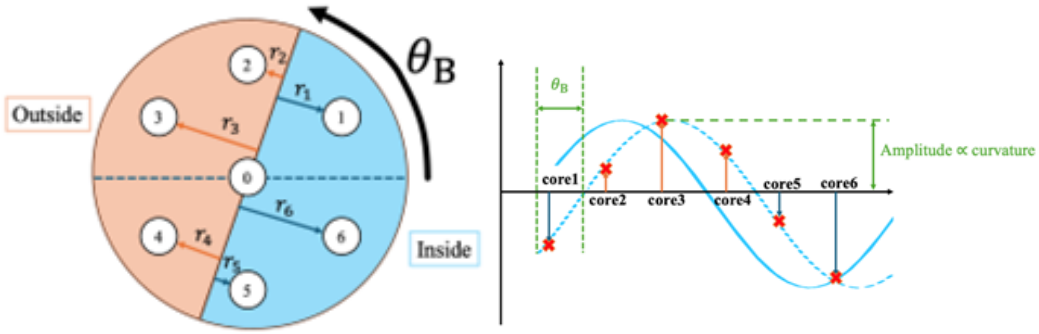

(a) (b)

Figure 3 (a) Cross-section of multicore FBG (MCFBG) and (b) relative Bragg wavelength shift of FBGs in peripheral cores

2.5 Design concept of the bending sensor using I-OFDR and TPA in Si-APD

Figure 4 illustrates the optical fiber bending sensor design concept based on the two-photon absorption (TPA) response of a Si-APD and the I-OFDR technique. Unlike conventional multidetector systems, this system can distinguish multiple cores using a single photodetector (Si-APD). To detect the position of the Bragg gratings and the intensity of the reflected light, the probe and reference beams are intensity-modulated using a chirped signal. The chirped signal can be generated by a commercially available signal generator in the actual experimental setup. Simultaneously, the wavelength of the probe light is swept to measure the reflection spectrum. A lock-in amplifier detects the two-photon absorption photocurrent from the Si-APD, and the resulting signal is observed in real time with a spectrum analyzer. The experiment was conducted under vibration-free conditions at room temperature. Therefore, FBGs were not affected by factors other than bending. This configuration enables real-time bending measurement.

3. Results and Discussion

We conducted a proof-of-concept experiment to validate the proposed sensing system based on incoherent optical frequency domain reflectometry (I-OFDR) and the two-photon absorption (TPA) process in a Si-APD. The experiment was performed by placing the optical fiber along the circumference of printed circles with radii of 5, 6, 7, 8, and 9 cm on paper and manually bending

the fiber to match the circular arcs. Table 1 shows the estimated curvature radii obtained for each target bending radius and the errors between them. Figure 5 presents the sinusoidal curve fitting of the relative Bragg wavelength shifts measured in each core of a MCFBG when the bending radius was 7 cm. The amplitude of the sine curve fitted by plotting the Bragg wavelength shift of each core relative to core 0 represents the curvature radius according to equations (8) and (10). The estimated curvature radius was 7.15 cm from the fitting results, which sufficiently demonstrates the feasibility of the design concept. The errors for each target bending radius were comparable. A maximum error of 0.19 cm is considered reasonable, given the radius error of the curve drawn on the paper and the positioning error caused by manual fiber setting. In this experiment, the wavelength sweep time was 25 s, which represents the system's effective measurement time.

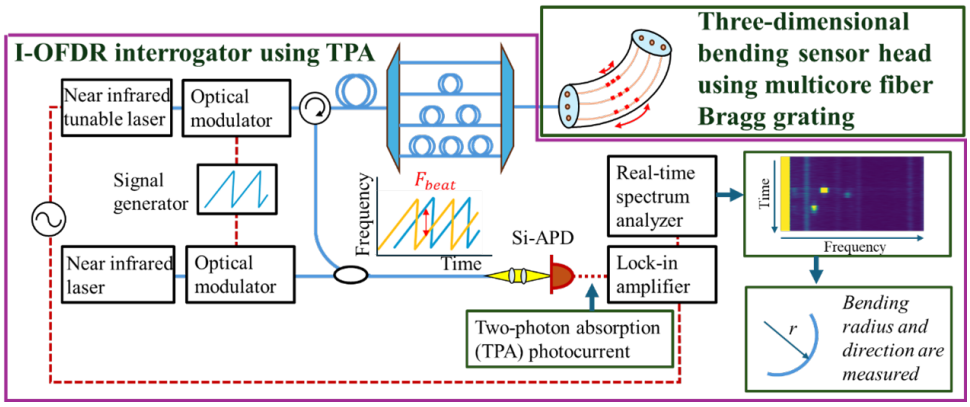

Figure 4 Design concept of the proposed bending sensor based on I-OFDR and TPA in Si-APD

Table 1 Actual and estimated bending radii and measurement errors

Curvature radius / cm	Estimated curvature radius /cm	Error / cm
9	9.19	0.19
8	7.97	0.03
7	7.15	0.15
6	5.96	0.04
5	5.16	0.16

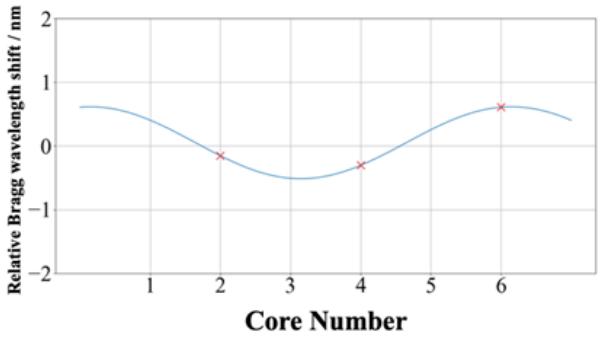

Figure 5 Sinusoidal curve fitting of the relative Bragg wavelength shift of the grating in each core

4. Conclusions

In this study, we proposed and demonstrated a novel design concept for a fiber-optic bending sensor based on I-OFDR and the Si-APD TPA process. The system uses intensity-modulated probe and reference beams with chirped signals, enabling the simultaneous detection of Bragg grating positions and reflection spectra. The sensing architecture is significantly simplified by leveraging the nonlinear TPA process, eliminating the need for high-speed photodetectors and complex electrical circuits. In this experiment, the measurement time was 25 s, which is significantly shorter than that of conventional methods. A proof-of-concept experiment was conducted using an MCFBG bent along a circular arc. The measured Bragg wavelength shifts were successfully fitted with a sinusoidal curve, and the estimated curvature radius closely matched the actual bending radius, validating the effectiveness of the proposed sensing approach. These results confirm that the integration of I-OFDR and TPA in Si-APD provides a practical and scalable solution for real-time, direction-sensitive fiber-optic bending measurement. The proposed method offers promising potential for applications in structural health monitoring, biomedical sensing, and robotics.

Acknowledgements

his work was supported by the Japan Society for the Promotion of Science (JSPS) KAKENHI Grant Number JP24K00894.

Author Contributions

Yuta Kurihara: Conceptualized and designed the study, developed the methodology, conducted the experiments, performed data analysis, and drafted the manuscript. Shinta Tsuzuki: Conducted experiments and contributed to data collection. Takuma Serizawa: Contributed to methodology development, assisted in experimental setup, and participated in data collection. Yosuke Tanaka: Proposed the research idea, supervised the project, contributed to conceptualization, assisted in manuscript drafting, provided critical revisions and editing, and served as the corresponding author.

Conflict of Interest

The authors declare no conflict of interest.

References

Allsop, T., Dubov, M., Martinez, A., Floreani, F., Khrushchev, I., Webb, D. J., & Bennion, I. (2006). Bending characteristics of fiber long-period gratings with cladding index modified by femtosecond laser. *Journal of Lightwave Technology*, *24*(8), 3147–3154. https://doi.org/10.1109/JLT.2006.878037

Barrera, D., Gasulla, I., & Sales, S. (2015). Multipoint two-dimensional curvature optical fiber sensor based on a nontwisted homogeneous four-core fiber. *Journal of Lightwave Technology*, *33*(12), 2445–2450. https://doi.org/10.1109/JLT.2014.2366556

Ben Hassen, R., Lemmers, A., & Delchambre, A. (2023). Tri-axial force sensor in a soft catheter using fiber Bragg gratings for endoscopic submucosal dissection. *IEEE Sensors Journal*, *23*(20), 24626–24636. https://doi.org/10.1109/JSEN.2023.3313172

Budnicki, D., Parola, I., Szostkiewicz, Ł., Markiewicz, K., Hołdyński, Z., & Wojcik, G. (2020). All-Fiber Vector Bending Sensor Based on a Multicore Fiber With Asymmetric Air-Hole Structure. *Journal of Lightwave Technology*, *38*(23), 6685–6690. https://doi.org/10.1109/JLT.2020.3012769

Donko, A., Beresna, M., Jung, Y., Hayes, J., Richardson, D. J., & Brambilla, G. (2018). Point-by-point femtosecond laser micro-processing of independent core-specific fiber Bragg grat-

ings in a multi-core fiber. *Optics Express*, *26*(2), 2039–2044. https://doi.org/10.1364/OE.26.002039

Flockhart, G. M. H., MacPherson, W. N., Barton, J. S., Jones, J. D. C., Zhang, L., & Bennion, I. (2003). Two-axis bend measurement with Bragg gratings in multicore optical fiber. *Optics Letters*, *28*(6), 387–389. https://doi.org/10.1364/ol.28.000387

Fujiwara, E., Hayashi, J. G., da Silva Delfino, T., Jorge, P. A. S., & de Barros Cordeiro, C. M. (2019). Optical fiber anemometer based on a multi-FBG curvature sensor. *IEEE Sensors Journal*, *19*(19), 8727–8732. https://doi.org/10.1109/JSEN.2019.2923046

He, Z., & Liu, Q. (2021). Optical fiber distributed acoustic sensors: a review. *Journal of Lightwave Technology*, *39*(12), 3671–3686. https://doi.org/10.1109/JLT.2021.3059771

Henken, K. R., Dankelman, J., van den Dobbelsteen, J. J., Cheng, L. K., & van der Heiden, M. S. (2014). Error analysis of FBG-based shape sensors for medical needle tracking. *IEEE/ASME Transactions on Mechatronics*, *19*(5), 1523–1531. https://doi.org/10.1109/TMECH.2013.2287764

Hill, K. O., & Meltz, G. (1997). Fiber Bragg grating technology fundamentals and overview. *Journal of Lightwave Technology*, *15*(8), 1263–1276. https://doi.org/10.1109/50.618320

Hochberg, R. C. (1986). Fiber-optic sensors. *IEEE Transactions on Instrumentation and Measurement*, *IM-35*(4), 447–450. https://doi.org/10.1109/TIM.1986.6499114

Issatayeva, A., Amantayeva, A., Blanc, W., Tosi, D., & Molardi, C. (2021). Design and analysis of a fiber-optic sensing system for shape reconstruction of a minimally invasive surgical needle. *Scientific Reports*, *11*, 8609. https://doi.org/10.1038/s41598-021-88117-7

Kersey, A. D., Davis, M. A., Patrick, H. J., LeBlanc, M., Koo, K. P., Askins, C. G., Putnam, M. A., & Friebele, E. J. (1997). Fiber grating sensors. *Journal of Lightwave Technology*, *15*(8), 1442–1463. https://doi.org/10.1109/50.618377

Khan, F., Denasi, A., Barrera, D., Madrigal, J., Sales, S., & Misra, S. (2019). Multi-core optical fibers with Bragg gratings as shape sensor for flexible medical instruments. *IEEE Sensors Journal*, *19*(14), 5878–5884. https://doi.org/10.1109/JSEN.2019.2905010

Li, H., Li, D., & Song, G. (2004). Recent applications of fiber optic sensors to health monitoring in civil engineering. *Engineering Structures*, *26*(11), 1647–1657. https://doi.org/10.1016/j.engstruct.2004.05.018

Li, L., He, R., Soares, M. S., Savović, S., Hu, X., & Marques, C. (2021). Embedded FBG-Based Sensor for Joint Movement Monitoring. *IEEE Sensors Journal*, *21*(23), 26793–26798. https://doi.org/10.1109/JSEN.2021.3120995

Lindley, E., Min, S.-S., Leon-Saval, S., Cvetojevic, N., Lawrence, J., Ellis, S., & Bland-Hawthorn, J. (2014). Demonstration of uniform multicore fiber Bragg gratings. *Optics Express*, *22*(25), 31575–31581. https://doi.org/10.1364/OE.22.031575

Liu, Y., Li, L., He, R., Soares, M. S., Savović, S., Hu, X., & Marques, C. (2019). Quasi-Distributed Directional Bending Sensor Based on Fiber Bragg Gratings Array in Triangle-Four Core Fiber. *IEEE Sensors Journal*, *19*(22), 10728–10735. https://doi.org/10.1109/JSEN.2019.2931916

Liu, Y., Williams, J. A. R., & Bennion, I. (2000). Optical bend sensor based on measurement of resonance mode splitting of long-period fiber grating. *IEEE Photonics Technology Letters*, *12*(5), 531–533. https://doi.org/10.1109/68.841276

Lyu, C., Li, P., Zhang, J., & Du, Y. (2025). Fiber optic sensors in tactile sensing: a review. *IEEE Transactions on Instrumentation and Measurement*, *74*, 7001816. https://doi.org/10.1109/TIM.2025.3527487

Madani, N. A., Purnamaningsih, R. W., Poespawati, N. R., Hamidah, M., Rahardjo, S., & Wibowo, D. K. (2023). Detection of Low Hydrostatic Pressure Using Fiber Bragg Grating Sensor. *International Journal of Technology*, *14*(7), 1527–1536. https://doi.org/10.14716/ijtech.v14i7.6714

Moore, J. P., & Rogge, M. D. (2012). Shape sensing using multi-core fiber optic cable and parametric curve solutions. *Optics Express*, *20*(3), 2967–2973. https://doi.org/10.1364/OE.20.002967

Nor, M. S. M., Khan, A. A., Mohamad, S., & Thirunavakkarasu, P. (2023). Development of Optical Fiber Sensor for Water Salinity Detection. *International Journal of Technology*, *14*(6), 1247–1255. https://doi.org/10.14716/ijtech.v14i6.6650

Pevec, S., & Donlagić, D. (2019). Multiparameter fiber-optic sensors: a review. *Optical Engineering*, *58*(7), 072009. https://doi.org/10.1117/1.OE.58.7.072009

Riza, M. A., Go, Y. I., Harun, S. W., & Maier, R. R. J. (2020). FBG sensors for environmental and biochemical applications—A review. *IEEE Sensors Journal*, *20*(14), 7614–7627. https://doi.org/10.1109/JSEN.2020.2982446

Roesthuis, R. J., Kemp, M., van den Dobbelsteen, J. J., & Misra, S. (2014). Three-dimensional needle shape reconstruction using an array of fiber Bragg grating sensors. *IEEE/ASME Transactions on Mechatronics*, *19*(4), 1115–1126. https://doi.org/10.1109/TMECH.2013.2269836

Sato, R., Takagi, R., Saito, I., Sonoda, N., Zhaoa, S., & Tanaka, Y. (2022). Multipoint FBG sensing using incoherent OFDR and two-photon absorption process in Si-APD. *Conference on Lasers and Electro-Optics (CLEO) 2022*, JW3B.94. https://doi.org/10.1364/CLEO_AT.2022.JW3B.94

Sonoda, N., Takagi, R., Saito, I., Abe, T., Zhao, S., & Tanaka, Y. (2021). Multipoint bending measurement using multicore fiber Bragg grating and two-photon absorption process in Si-APD. *IEEE Sensors Journal*, *21*(22), 25736–25742. https://doi.org/10.1109/JSEN.2021.3117858

Tanaka, Y., Abe, T., & Miyazawa, H. (2019). Directional curvature sensing using multicore fiber Bragg grating and two-photon absorption process in Si-APD. *Conference on Lasers and Electro-Optics (CLEO)*, SF3L.1. https://doi.org/10.1364/CLEO_SI.2019.SF3L.1

Tanaka, Y., & Miyazawa, H. (2017). Multipoint fiber Bragg grating sensing using two-photon absorption process in silicon avalanche photodiode. *Journal of Lightwave Technology*, *36*(4), 1032–1038. https://doi.org/10.1109/JLT.2017.2771513

Tanaka, Y., Nemoto, M., & Yamada, Y. (2017). Displacement measurement using two-photon absorption process in Si-avalanche photodiode and fiber Bragg gratings. *Journal of Lightwave Technology*, *36*(4), 1192–1196. https://doi.org/10.1109/JLT.2017.2760890

Tsuzuki, S., Sato, R., & Tanaka, Y. (2024). Simultaneous measurement of Bragg gratings' reflection spectra and their positions in multicore fiber using two photon absorption process in Si-APD. *Conference on Lasers and Electro-Optics Pacific Rim (CLEO-PR) 2024*, Mo3G–3.

Vilches, S., Zappe, H., & Ataman, Ç. (2023). Multi-point fiber-optic distance sensor for endoscopic surgery monitoring. *IEEE Photonics Technology Letters*, *35*(16), 883–886. https://doi.org/10.1109/LPT.2023.3270628

Wang, H., Zhang, R., Chen, W., Liang, X., & Pfeifer, R. (2016). Shape detection algorithm for soft manipulator based on fiber bragg gratings. *IEEE/ASME Transactions on Mechatronics*, *21*(6), 2977–2982.

Yang, S., Wang, H., Yuan, T., Zhang, X., & Yuan, L. (2022). Highly Sensitive Bending Sensor Based on Multicore Optical Fiber With Diagonal Cores Reflector at the Fiber Tip. *Journal of Lightwave Technology*, *40*(17), 6030–6036. https://doi.org/10.1109/JLT.2022.3184042

You, J., Shan, M., Sugita, Y., Cheng, Z., Abe, I., & Iiyama, K. (2025). Multipoint fbg sensing system for long-range and long-term structural health monitoring by incoherent fmcw optical ranging system. *IEEE Sensors Journal*, *25*(12), 21608–21616. https://doi.org/10.1109/JSEN.2025.3564040

Yue, X., Lu, R., Yang, Q., Song, E., Jiang, H., & Ran, Y. (2023). Flexible Wearable Optical Sensor Based on Optical Microfiber Bragg Grating. *Journal of Lightwave Technology*, *41*(6), 1858–1864. https://doi.org/10.1109/JLT.2022.3227186